INTEGRATED POLARIZATION ANALYZING CMOS IMAGE SENSOR FOR AUTONOMUS NAVIGATION USING POLARIZED LIGHT

Mukul Sarkar[1, 2], David San Segundo Bello[1], Chris van Hoof[1], Albert Theuwissen[2, 3]
[1]imec, [2]Delft University of Technology, [3]Harvest Imaging
Mukul.Sarkar@imec-nl.nl

Abstract—**Navigation is important both for insects to perform living tasks and robots to perform assigned tasks. We propose a CMOS image sensor for autonomous agent navigation which mimicks the navigational patterns of insects using the variations in the degree of skylight polarization. The polarization pattern of the skylight varies in a systematic way both in the plane (e-vector) and the degree of polarization according to the sun's position. The proposed CMOS image sensor is able to sense polarization information in real time using a metallic wire grid micro-polarizer oriented in various directions on top of the pixel. The degree of polarization is computed from the sensed polarization information, the variations of which can be used as a compass. The image sensor consist of an array of 128x128 pixels, occupies an area of 5x4mm^2 and it has been designed and fabricated in a 180nm CMOS process.**

I. INTRODUCTION

There are two types of spatial representation created by navigation. One type is a cognitive map or survey representation of space and the other is a route representation [1], [2]. In the route representation, the navigator tries to learn the points in the route. Cognitive maps on the other hand represent the geometric layout of the topography of a space. The cognitive maps basically define the Euclidean relations (straight line distance and direction) among relevant landmarks within a coordinate reference system centered on the environment.

The role of vision in navigation and cognitive mapping has been extensively studied [3]. Based on the cognitive mapping, navigation can be broadly classified into geocentric and egocentric. In geocentric navigation, one uses its cognitive map and its orientation with respect to geocentric coordinates in order to set a course to a goal. Visual cues such as landmarks become very important to generate the cognitive maps. Egocentric navigation on the other hand relies on path integration, where the movement cues of the navigator are continuously integrated. Animals using egocentric navigation are able to track distance and direction in order to estimate their position without relying on visual landmarks.

Humans navigate using geocentric navigation. In the absence of information about the location of nearby objects in the environment, humans have difficulty monitoring their travel trajectories, even for short paths. The ability of insects to navigate effortlessly in complex environments without stressing their nervous system has been a subject of research in robotics. One remarkable and well studied model is that of the Saharan desert ant (Cataglyphis fortis). Cataglyphis fortis are excellent navigators and perform mostly egocentric navigation [4]. These ants measure the direction by using skylight cues as compass, and the distance is measured by counting the step size [4]–[7]. It is further suggested by Fent [8], that besides the e-vector[1] orientation of the skylight, ants also use its degree of polarization, which remains constant for a particular position of the sun and varies as the sun moves. This makes their navigation pattern completely independent of external visual cues.

The cheap computational strategies that insects use to navigate have been modeled by various researchers. Lambrinos et al. [9], [10] modeled the polarized light sensitive receptors (POL-neurons) in the Cataglyphis using a pair of photodiodes with a linear polarizer on top. Kane et al. [11] proposed a much simpler method where a normal camera with a linear polarization filter is used to take two images, the second image taken with the polarization filter set orthogonal with respect to its position in the first image. From these two images a mean intensity function as a function of polarization angle was derived similar to the form proposed by Lambrinos et al. [10] for the photosensitive diodes.

Lambrinos et al. in their robots has successfully demonstrated compass detection capability. However a important disadvantage of their system is the use of three cameras to detect the direction. Three cameras with 0º, 60º and 120º orientations have to be monitored which is expensive in terms of cost, area, complexity of the algorithm and also the computation power needed to implement the algorithms. The system by Kane et al. also suffers from the disadvantage of using an external linear polarizer which needs to be rotated to have three images with three different transmission axis of the linear polarizer. Both systems are also not very well compensated for the change in the degree of polarization during the day. The systems also need an ephemeris compensation algorithm. The ephemeris function is a function that describes the change of the sun azimuth over time and it depends on the season and the geographical latitude. It is known that the rate of change of the sun's azimuth is not constant: it is faster around noon and slower in the morning. Insects such as bees and ants also suffer from the inherent changes in the ephemeris function but are known to refine its compass detection ability with experience.

The polarization antagonism prevalent in the compound eye of insects detects the direction of their travel using polarization of the skylight [9]. Another advantage of the compound eye is the wide field of view which leads to near

[1] e-vector is the electric field vector of the polarized light in the sky.

978-1-4244-5164-7/10/$26.00 ©2010 IEEE

panoramic vision. The field of view in the case of insects is spherical in nature and is advantageous in detection of self-motion [12]. This is really exciting as an application of low power imaging, which is becoming a very important research area in the electronic imaging world. Current sensors employed for navigation applications, and especially for robotic navigation, use a generalized algorithm of capturing 2D images using a standard CMOS or CCD camera and then processing those captured images for vector calculations to determine the motion vector and the direction vector [13]. This is very processing intensive and power consuming.

The polarization information in real time can be obtained with a photodetector array, such as a CMOS or a CCD sensor array and a single or multi-axis micropolarizer filter array coupled to it. The polarization filter can be either externally coupled, or an organic micro-polarizer or a metallic wire grid micro-polarizer. The main advantage of both the external polarizer and the organic micro-polarizer is their high extinction ratio[2]. On the other hand the former needs to be mechanically controlled while the latter needs additional fabrication steps which are currently not compatible with standard CMOS technology. The metallic wire grid micro-polarizer is simple to fabricate using the metal layers available with standard CMOS technologies. We have demonstrated an embedded wire grid polarizer with measured extinction ratios of 6.3 and 7.7, using a wire grid pitch of 0.48 μm [14].

In this work we present a CMOS image sensor for autonomous agent navigation using the real time polarization information obtained using the embedded metallic wire grid micro-polarizer. The variations in the degree of polarization and the polarization Fresnel ratio with changes in the angular position of the incoming polarized light ray are shown to work as an effective compass. Section II gives a brief overview of the theory related to polarization. Section III describes the designed image sensor with two polarization sense regions embedded with micropolarizers created using a metallic wire grid. Section IV presents the measurement results, which show that the variations in the degree of polarization and polarization Fresnel ratio with the variation in the polarization angle of the incoming light ray are effective as compass. Section V concludes the paper.

II. THEORY

A. Stokes parameters and degree of polarization

Electromagnetic radiation travels as transverse waves, i.e., waves that vibrate in a direction perpendicular to their direction of propagation. The mathematical representation of a plane wave propagating in the z direction is given by equation [1.0]

$$E = E_0 \cos(kz - \omega t + \varphi_0) \,. \qquad [1.0]$$

Where E_0 is the amplitude, k is the propagation (or wave) constant ($k=2\pi/\lambda$), ω is the circular frequency ($\omega=kc= 2\pi c/\lambda$) and φ_0 is the initial phase.

Polarization is the distribution of the electric field in the plane normal to the propagation direction. In an unpolarized or randomly polarized electromagnetic wave the orientation of the electric field vector changes randomly. Three states of polarization of a light wave are possible: completely unpolarized, completely polarized or partially polarized. An unpolarized electromagnetic wave can be polarized through absorption, reflection, refraction and scattering.

The electric field of an electromagnetic wave polarized by scattering consists of a polarized and an unpolarized component. The polarization state of an electromagnetic wave can be conveniently described by a set of parameters called Stokes parameters which were developed by G.G. Stokes in 1852. The four Stokes parameters are grouped into a column vector, known as Stokes vector, as shown in equation [1.1]. The Stokes parameters represented in equation [1.1] are Intensity (I), degree of polarization (Q), plane of polarization (U) and ellipticity (V). The first Stokes parameter describes the total intensity of light, while the other parameters describe the polarization state of the light. For unpolarized light $Q=U=V=0$,or equivalently $S_1=S_2=S_3=0$.

$$\vec{S} = \begin{bmatrix} S_0 \\ S_1 \\ S_2 \\ S_3 \end{bmatrix} = \begin{bmatrix} I \\ Q \\ U \\ V \end{bmatrix} \qquad [1.1]$$

There are two ways to express the partial polarization of the electromagnetic wave: the degree of polarization (*DOP*) and the Jones coherency matrix (J). The degree of polarization is a measure of the percentage of the electric field of the light which is polarized compared to the electric field of the total incident light. *DOP* is a scalar value, and will be used to express the partial polarization in this work [15]. In a linearly polarized light beam, circular and elliptical polarizations do not usually occur. Its degree of polarization is thus often referred to as degree of linear polarization (*DOLP*). In terms of Stokes parameters, the DOLP of the light wave is expressed as [16]:

$$DOLP = \delta = \frac{S_1}{S_0} \qquad [1.2]$$

The Stokes parameters S_1 and S_2 are calculated as:

$$\begin{aligned} S_0 &= I_{90^\circ}^2 + I_{0^\circ}^2 \\ S_1 &= I_{90^\circ}^2 - I_{0^\circ}^2 \end{aligned} \qquad [1.3]$$

Where I_{0° is the intensity of the light after passing through a horizontal linear polarizer, I_{90° is the intensity after a vertical linear polarizer.

[2] The extinction ratio is defined as the ratio of the power of a parallel plane-polarized to the power of a perpendicular plane-polarized light beam.

The DOP is also related to the maximum and minimum transmitted intensities [17] as shown in equation [1.4]

$$DOP = \delta(x,y) = \frac{I_{\max}(x,y) - I_{\min}(x,y)}{I_{\max}(x,y) + I_{\min}(x,y)} \quad [1.4]$$

Where $I_{max}(x,y)$ and $I_{min}(x,y)$ are the maximum and minimum transmitted intensities for the pixel at coordinates x and y. The maximum transmittance in a polarizer is achieved when the polarization axis is parallel to the polarization of the incoming light, while minimum transmittance occurs when the polarization axis is perpendicular to the polarization of the incoming light. This is described by the Law of Malus which states that transmission is proportional to the square of the cosine of the angle between the plane of polarization of the input light and the transmission axis of the polarizer.

The DOP in its simplest form is represented by Polarization Fresnel Ratio (*PFR*) described by Wolff [17]. The *PFR* is the ratio of the perpendicular Fresnel coefficient to the parallel Fresnel coefficient. The Fresnel coefficients describe the reflection and transmission coefficients of the light wave at an interface. The *PFR* can be roughly estimated as:

$$\delta = \frac{Power\ of\ the\ perpendicular\ polarization}{Power\ of\ the\ parallel\ polarization} = \frac{P_{per}}{P_{par}} \quad [1.5]$$

III. SENSOR DESCRIPTION

The image sensor consists of an array of 128 by 128 pixels and it occupies an area of 5 x 4 mm^2. It has been designed and fabricated in the 180nm CMOS CIS process from UMC. The polarization sensing sensor has an embedded linear wire grid polarizer in each pixel, realized with the first metal layer of the process on top of a pinned photodiode (p^+/n^-/p-sub). The linear wire grid polarizer was implemented using thin metal strips with a line/space of 240nm/240nm (pitch of 480nm) as shown in figure 1.

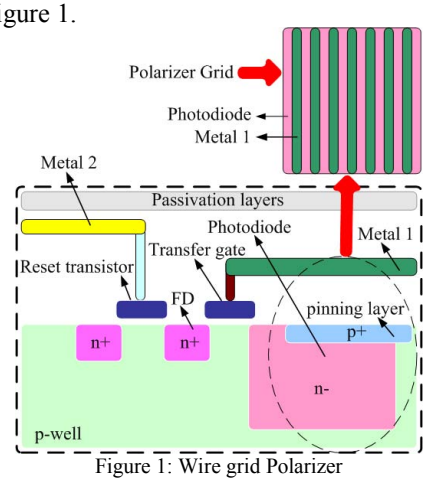

Figure 1: Wire grid Polarizer

Table 1 lists the sensor specifications and figure 2 shows the sensor architecture.

TABLE 1: Sensor specifications

Process	0.18µm 1 poly 3 metals UMC CIS process
On-chip Polarizer	Line/Space = 240nm/ 240nm (480nm pitch)
Active imager size	3.2 mm(H) x 3.2 mm(V)
Chip Size	4 mm(H) x 5 mm(V)
Active pixels	128 x 128
Pixel size	25µm x 25µm
Shutter type	Global shutter
Maximum data rate/master clock	64 MPS / 32 MHz
Supply voltage	1.8V

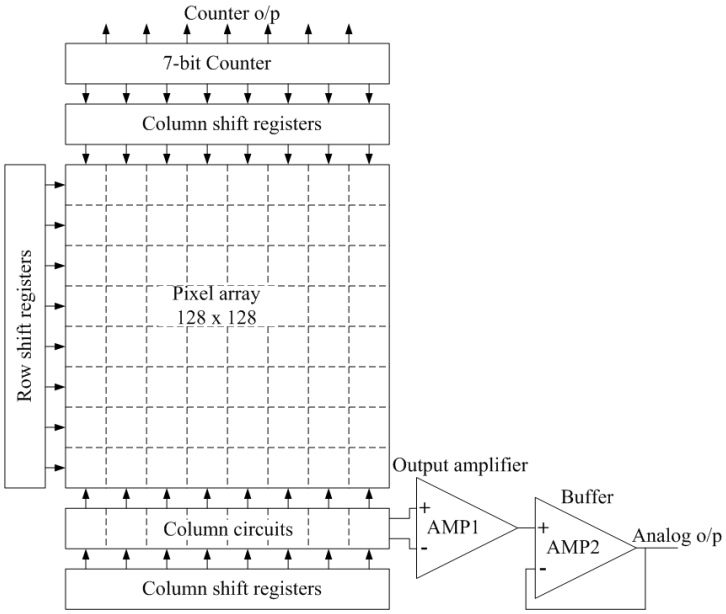

Figure 2: Sensor architecture

The chip is divided into four main blocks. The first one consists of the pixel array with the photodiodes and the associated circuitry for analog computations. Each pixel contains a pinned photodiode and 32 transistors to perform low level image processing[3]. The size of the photodiode is 10µm x 10µm which corresponds to a 16% pixel fill factor. Second, placed below the pixel array is the analog readout circuit. The analog readout circuit consists of column level circuits for double differential sampling, an output amplifier, a buffer and the column shift register. Third, placed at the top is the digital readout circuit. The digital readout circuit consists of a 7-bit counter and a column shift register. The 7-bit counter is used to count the number of active high pixels in each row. Finally, the left side is dedicated to a row select logic and timing control blocks to address each row of pixels sequentially.

[3]In this paper we focus on the polarization sensing ability of the sensor thus the low level image processing will not be discussed.

The array of 128 by 128 pixels was split into three regions as shown in figure 3:

1. A 64x128 array without a metal grid used for normal imaging applications
2. A 64x64 array (polarization sense region 1) consisting of 2 by 2 pixel arrays where two pixels (A and B) measure the intensity while the other two measure the 0º (D), and 90º (C) polarized intensity, respectively
3. A 64x64 array (polarization sense region 2) consisting of 2 by 2 pixel arrays where one pixel records the intensity of the light (A) while the other 3 record the 0º (B), 45º (C) and 90º (D) polarized intensity.

The additional pixel sensitivity to 45º polarized light in sense region 2 is used to compute the Stokes parameters. The pixels dedicated to sense the intensity in regions 1 and 2 are used to normalize the data obtained from the pixels sensitive to polarization directions.

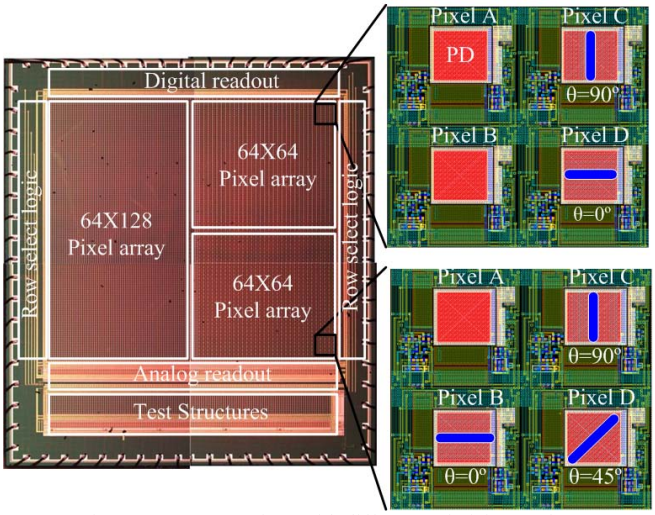

Figure 3: Sensor Regions with different Polarizing angles.

IV. PERFORMANCE ANALYSIS

The measurement setup is shown in figure 4.

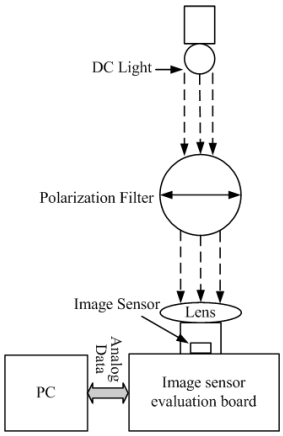

Figure 4: Measurement setup

The DC light source generates unpolarized light which is polarized by transmitting through a linear polarizer. The linear polarized light intensity is then sensed by the imager and the analog output of the imager is fed to the PC for processing of the sensed data. The corresponding analog outputs of the pixels sensitive to 0º, 45º and 90º in the polarization sense regions are used to compute the Stokes parameters. For the first version of the sensor the Stokes parameters were computed off-chip to have a proof of concept. The circuits required for the computation of Stokes parameters and other digital processing for the implementation of the algorithm can easily be integrated on chip. Control pulses for the image sensor are generated by an FPGA, so that the accumulation and readout timing can be manipulated by an appropriate VHDL program.

An average value of the intensities of the pixel sensitive to 0º and 90º in the sense region 1 and 0º, 45º and 90º in the sense region 2 is computed for 30 frames using the equation [1.6].

$$p_{avg(With\ \ linear\ \ polarizer)}(x,y) = \frac{1}{N}\sum_{n=1}^{N} p(x,y) \qquad [1.6]$$

Where $p(x,y)$ is the measured pixel intensity, x and y are the row and column number of the sensor array and N is the number of frames selected. At the beginning of the experiment the mean of the chosen pixel array of 20x20 without the linear polarizer is noted as in equation [1.7]. This value will be used as a normalization factor.

$$p_{avg(Without\ \ linear\ \ polarizer)}(x,y) = \frac{1}{XYN}\sum_{n=1}^{N}\sum_{x=0}^{X-1}\sum_{y=0}^{Y-1} p(x,y) \qquad [1.7]$$

Where X and Y are the pixel array dimensions and N is the total number of frames used to compute the mean. The normalized intensity is then obtained by dividing the mean pixel intensity with the linear polarizer (equation [1.6]) by the mean pixel intensity without the linear polarizer (equation [1.7]) shown in equation [1.8].

$$Normalized\ p_{avg}(x,y) = \frac{\left(\frac{1}{N}\sum_{n=1}^{N} p\ (x,y)\right)}{\left(\frac{1}{XYN}\sum_{n=1}^{N}\sum_{x=0}^{X-1}\sum_{y=0}^{Y-1} p(x,y)\right)} \qquad [1.8]$$

The normalized pixel intensities for 0º and 90º polarization sensitive pixels in sense regions 1 and 2 are shown in figure 5. For both polarization sense regions the 0º linear polarizer has the maximum at 0º and the minimum at 90º. Similarly, for the 90º polarizer the maximum is observed at 90º and the minimum at 0º.

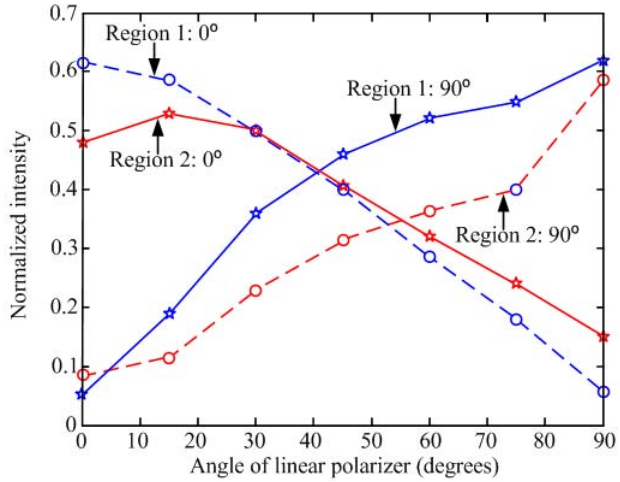

Figure 5: Normalized intensity obtained for 0º and 90º polarization sensitive photodiode in sense region 1 and 2.

The logarithmic difference of the two linear polarizations mean outputs was computed off chip and is shown in figure 6. A very similar characteristic as the one shown by Lambrinos et al. [9], [12] was achieved for both sense regions.

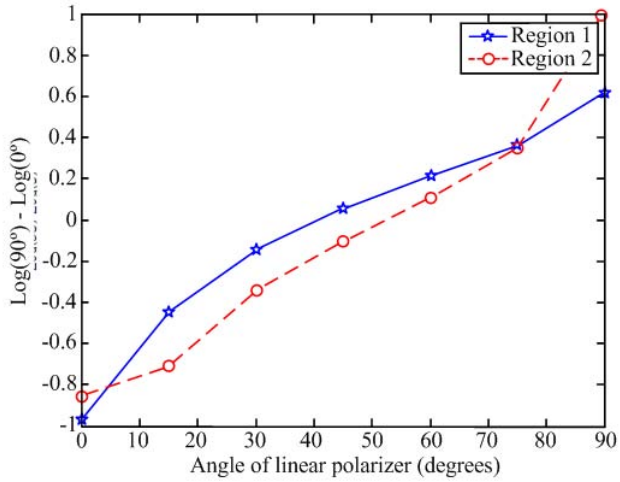

Figure 6: The logarithmic difference of the orthogonal signals in sense region 1 and 2

For both polarization sense regions, the logarithmic difference of the two orthogonal signals was found to have a minimum at 0º linear polarizer angle and a maximum at 90º linear polarizer angle. The logarithmic difference shows an approximately linear increase for increasing linear polarizer angle. This variation in the logarithmic difference can be conceptually used to determine the angle of linear polarization, and based on a reference or look-up table it can be used as a compass.

The image intensity from the photodiodes in the models of both Lambrinos et al. and Kane et al. is a function of the degree of polarization which changes over the course of the day. Lambrinos et al. offsets the effects of the variation in the degree of polarization by normalizing the output and Kane et al. did not compensate for it. We take a different approach and instead of focusing on polarization differential image or polarization summation image, we study the variation in the degree of polarization with respect to the orientation. We evaluate the degree of polarization behavior with the orientation angle and assert that this degree of polarization information can be used to extract the orientation angle and hence serve as a compass clue.

The variations in the degree of polarization [12] in an image $f(\varphi)$ for changes in the orientation angle φ with respect to the solar meridian is given by equation [1.9]. An inverse relationship between the degree of polarization d and the orientation angle φ is obtained.

$$d = \frac{1}{\cos(2\phi)}\left[1 - \frac{f(\phi)}{KI}\right] \qquad [1.9]$$

Where I is the total intensity, $I=I_{max}+I_{min}$ where I_{max} is the maximum and I_{min} is the minimum intensity obtained from the photodiodes with linear polarizer in crossed-analyzer configuration, d is the degree of polarization, φ is the orientation with respect to the solar meridian maximizing $f(\varphi)$ (tuned to e-vector direction), $f(\varphi)$ is the mean intensity of an image and K is a constant [18].

The Stokes degree of linear polarization calculated from equation [1.2] is plotted in figure 7. The DOP calculated using the maximum and minimum transmittance (equation [1.4]) is also shown in figure 7. The graph shows the inverse relationship between orientation angle or the angle of linear polarizer and the degree of linear polarization.

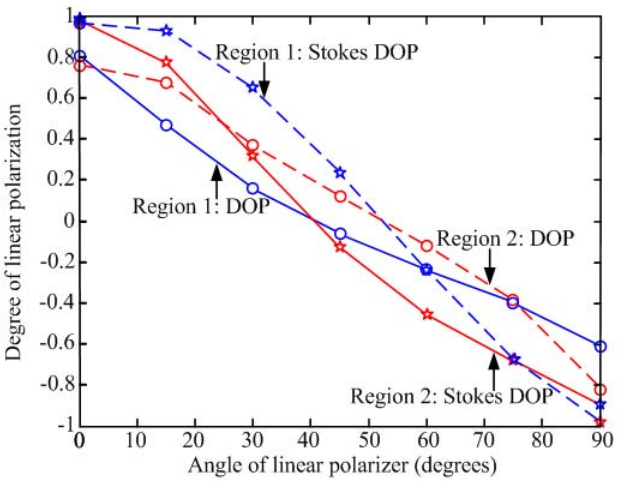

Figure 7: Degree of linear polarization for sense region 1 and 2.

Figure 7 shows that both the DOLP obtained either by the Stokes parameters and the DOP obtained with the maximum and minimum transmittance varies from +1 to -1 as the polarizer angle is varied from 0º to 90º. The variation obtained in the degree of linear polarization with respect to the orientation angle can be used as a compass. This approach has the advantage of using fewer computations than the model proposed by Lambrinos et al., where at first the system output was logarithmized and then anti-logarithamized and normalized for the removal of the dependence on the degree of

polarization. In the proposed model it is also possible for on-chip computations of the degree of polarization, which makes the system simpler and easier to integrate.

A further simplification to obtain the degree of polarization is to calculate the *PFR* as described by equation [1.5]. The pixel intensities obtained from the pixels covered with wire grid polarizer tilted by 0º and 90º in both sense regions is used to compute the *PFR*. The variation in the *PFR* with varying angle of linear polarizer is shown in figure 8.

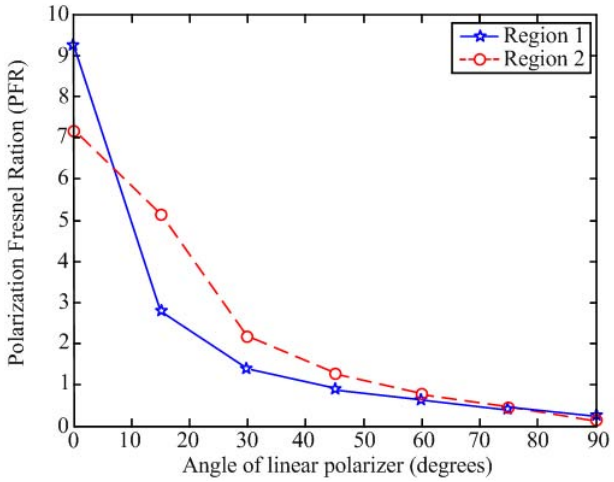

Figure 8: Polarization Fresnel Ratio (PFR) for sense region 1 and 2.

From figure 8, it is observed that the *PFR* has a maximum when the polarizer angle is 0º and steadily decreases to a minimum when the polarizer angle is 90º. The fall off is steep for lower angle of the linear polarizer than for the higher values. Although the variations in the *PFR* with varying polarizer angle are not linear, the variation for various angles of linear polarizer is still suitable to be used as compass to detect the direction of the incoming polarized light ray. The division of the two polarization amplitudes can be done with an analog divider circuit, simplifying the integration and making PFR a very good tool to derive compass information.

V. CONCLUSION

A polarization navigation sensor for autonomous agent navigation using the polarized component of the light was presented. The sensor working principle is based on the insect's principle form of egocentric navigation. The designed image sensor has the capability to sense 0º, 45º and 90º polarized light intensity, the intensities of which are used to compute the degree of polarization. The degree of polarization of the skylight for a given elevation of the sun is a constant, and this principle can be used as a compass clue. Though this principle is very common in insects, to our knowledge it has not been explored in sensors yet. The variations in the polarization Fresnel ratio with the change in the angle of linear polarizer can also serve as a tool for compass. The computational algorithm can be implemented on-chip which would result in miniaturized navigational sensors in future.

ACKNOWLEDGMENT

The authors would like to thank DALSA for providing the test table to characterize the sensor, INVOMEC for helping with the fabrication of the chip, A. Mierop of DALSA, G. Meynants of CMOSIS and P. Merken for their valuable contributions to the project.

REFERENCES

[1] John O'keefe and Lynn Nadel, "The Hippocampus as a Cognitive Map". Oxford University press, 1978

[2] P.W. Thorndyke and B. Hayes-Roth, "Differences in spatial knowledge acquired from maps and navigation". Cognitive Psychology, 14, 560-589, 1982.

[3] V.V. Hafner, "Adaptive Navigation Strategies in Biorobotics: Visual Homing and Cognitive Mapping in Animals and Machines". Shaker Verlag, 2004.

[4] R. Wehner B. Michel and P. Antonsen, "Visual navigation in insects: coupling of egocentric and geocentric information". J. of Experimental Bio. 199, 129-140, 1996.

[5] S. Sommer, and R. Wehner, "The ant's estimation of distance travelled: experiments with desert ants, Cataglyphis fortis". J. Comp. Physiol. A 190, 1-6, 2004.

[6] M. Müller and R. Wehner, "The hidden spiral: systematic search and path integration in desert ants, Cataglyphis fortis". J. Comp. Physiol. A 175, 525 - 530, 1994.

[7] R. Wehner and M. Mueller, "The significance of direct sunlight and polarized skylight in the ant's celestial system of navigation". PNAS, august 15, 2006, vol.103, no. 33, pages 12575-12579.

[8] K. Fent, "Polarized skylight orientation in the desert ant Cataglyphis". J. Comp. Physiol. A 158,145 -150, 1986.

[9] D. Lambrinos, R. Möller, T. Labhart, R. Pfeifer, R. Wehner, "A mobile robot employing insect strategies for navigation". Robotics and Autonomous Systems 30(1-2): 39-64 (2000).

[10] D. Lambrinos, M.Maris, H.Kobayashi, T. Labhart, R.Pfeifer and R. Wehner, "An Autonomous agent navigating with a polarized light compass", Adaptive behaviour, 6(1): 131-161, 1997.

[11] K. Usher, P. Ridley and P. Corke, "A Camera as a polarized light compass: preliminary experiments". Aust. Conf. on Robo. And Auto, 2001.

[12] C. Fermuller and Y. Aloimonos, "Ambiguity in structure from motion: Sphere versus plane". International Journal of Computer Vision, 28:137{154, 1998.

[13] Z. Chen and S. T. Birchfield, "Qualitative vision based mobile robot navigation". IEEE International Conf. on robotics and Automation (ICRA), Orlando, Florida, May 2006.

[14] M. Sarkar, S.S.B. David, C.V. Hoof, A.J.P. Theuwissen, "Polarization analyzing CMOS image sensor". ISCAS 2010, Paris (accepted)

[15] J.N. Damask, "Polarization optics in telecommunications". Springer, 2005, pp. 22.

[16] D. D. Malacara, "Physical optics and light measurements". Academic Press, 1989, pp.157.

[17] Lawrence B. Wolff, "Polarization based material classification from specular reflection", IEEE transactions on pattern analysis and machine intelligence, vol. 12, No. 11 Nov 1990.

[18] G.D. Bernard and R. Wehner, "Functional similarities between polarization vision and color vision". Vision Res, 17:1019-1028, 1977.